Received: 14 September 2021 | Accepted: 29 October 2021

DOI: 10.1111/1753-0407.13236

Journal of Diabetes

WILEY

ORIGINAL ARTICLE

Relationships between type 2 diabetes, cell dysfunction, and redox signaling: A meta-analysis of single-cell gene expression of human pancreatic α- and β-cells

Emily Sara Marques[1] | **Emily Formato**[2] | **Wenle Liang**[1] | **Emily Leonard**[1] | **Alicia R. Timme-Laragy**[1]

[1]Department of Environmental Health Sciences, University of Massachusetts Amherst, Amherst, Massachusetts, USA

[2]Molecular and Cellular Biology Graduate Program, University of Massachusetts Amherst, Amherst, Massachusetts, USA

Correspondence
Alicia R. Timme-Laragy, Department of Environmental Health Sciences, University of Massachusetts Amherst, School of Public Health and Health Sciences, Goessmann 171B/Morrill 1 N425, 686 North Pleasant St, Amherst, MA 01003-9298, USA.
Email: aliciat@schoolph.umass.edu

Funding information
US National Institute of Health, Grant/Award Numbers: 5R01ES025748-05, P42ES027706

Abstract

Background: Type 2 diabetes mellitus (T2DM) is a chronic disease characterized by insulin resistance and failure of β-cells to meet the metabolic demand for insulin. Recent advances in single-cell RNA sequencing (sc-RNA-Seq) have allowed for in-depth studies to further understand the underlying cellular mechanisms of T2DM. In β-cells, redox signaling is critical for insulin production. A meta-analysis of human pancreas islet sc-RNA-Seq data was conducted to evaluate how T2DM may modify the transcriptomes of α- and β-cells.

Methods: Annotated sc-RNA-Seq data from six studies of human pancreatic islets from metabolically healthy and donors with T2DM were collected. α- and β-cells, subpopulations of proliferating α-cells, immature, and senescent β-cells were identified based on expression levels of key marker genes. Each dataset was analyzed individually before combining, using weighted comparisons. Pathways of significant genes and individual redox-related gene expression were then evaluated to further understand the role that redox signaling may play in T2DM-induced β-cell dysfunction.

Results: α- and β-cells from T2DM donors modified genes involved in energy metabolism, immune response, autophagy, and cellular stress. α- and β-cells also had an increased nuclear factor erythroid 2-related factor 2 (NFE2L2)-mediated antioxidant response in T2DM donors. The proportion of immature and senescent β-cells increased in T2DM donors, and in immature and senescent β-cells, genes regulated by NFE2L2 were further upregulated.

Conclusions: These findings suggest that NFE2L2 plays a role in β-cell maturation and dysfunction. Redox singling maybe a key pathway for β-cell restoration and T2DM therapeutics.

KEYWORDS

meta-analysis, oxidative stress, RNA-Seq, transcriptome, type 2 diabetes mellitus

Highlights

- Meta-analysis of α- and β-cell transcriptomes reveals modified energy metabolism, immune response, autophagy, and cellular stress pathways in cells from type 2 diabetes mellitus.
- The proportion of immature and senescent β-cells is increased in islets from type 2 diabetes mellitus.
- α- and β-cells from type 2 diabetes mellitus have an increased nuclear factor erythroid 2-related factor 2 (NFE2L2)-mediated antioxidant response.
- Immature and senescent β-cells had increased NFE2L2-mediated antioxidant response, and this suggests that NFE2L2 plays a role in β-cell dysfunction and maturation.

1 | INTRODUCTION

According to estimates from the International Diabetes Federation atlas, 463 million people had diabetes worldwide in 2019, and this number is expected to climb to 700 million by 2045.[1,2] Type 2 diabetes mellitus (T2DM) is a chronic disease characterized by insulin (INS) resistance and severe β-cell dysfunction. β-cells, along with α, δ, ε, and υ cells make up the islets of Langerhans of the endocrine pancreas and are essential for maintaining glucose homeostasis. β-cells produce INS in response to elevated blood glucose, and α-cells secrete glucagon (GCG), which releases glucose from the liver and lipids from adipose tissue.[3] A key feature of T2DM is the failure of β-cells to meet the metabolic demand for INS, and recent advances in single-cell RNA sequencing (sc-RNA-Seq) have allowed for further understanding of the underlying mechanisms of islet cell maturation, maintenance, and dysfunction in T2DM.[4]

Many sc-RNA-Seq studies have found variable transcript enrichment across different islet cell types and rare cell subpopulations that can only be possible through sc-RNA-Seq.[5–12] In T2DM, α-cells may transdifferentiate to β-cells, under an extreme demand for INS, and also have been shown to increase proliferation via an elevated inflammatory response in T2DM and obesity.[13–15] β-cells from T2DM donors have been found to have altered β-cell immune response, cell cycle pathways, transcription factor expression, energy metabolism, and protein synthesis in several sc-RNA-Seq studies.[10–12] As reviewed by Salinno et al,[16] subpopulations of β-cells exist in a balance of proliferative capacity (immature cells)[17] or INS production (mature cells).[18] The ratio of mature and immature β-cells is thought to reflect the proliferative capability of β-cells.[19] Immature β-cells display high basal levels INS; however, it is unclear if they are capable of glucose-stimulated INS secretion.[20] Under healthy conditions, only a small pool of β-cells retain proliferative capabilities.[21] β-cell proliferation has been shown to increase with INS resistance in obesity,[22] and in the present study, the transcriptomes of subpopulations of proliferating α-cells, immature, and senescent β-cells will be evaluated in the context of T2DM.

A key feature in the pathophysiology of T2DM is glucotoxicity and lipotoxicity, which generate high amounts of reactive oxygen species (ROS) and oxidative stress. ROS generation, mitochondrial dysfunction, endoplasmic reticulum (ER) stress, and autophagy are all implicated in the development of T2DM and can impair β-cell function.[23,24] β-cells maintain low levels of antioxidant defenses and an oxidized redox state, which is necessary to form the three disulfide bonds in INS.[25–27] ROS also act as signaling molecules to guide cell fate and maturation in β-cells.[28–30] The induction of antioxidant enzymes via nuclear factor erythroid 2-related factor 2 (NFE2L2) provides protection from oxidative damage; however, induction of NFE2L2 may also blunt glucose-triggered ROS signaling, thus reducing INS secretion.[30] Recently an alternative pathway of NFE2L2 activation has also been described, where blockage of autophagosome-lysosome fusion leads to sequestosome 1 (SQSTM1)-mediated sequestration of Kelch-like epichlorohydrin (ECH)-associated protein 1 (KEAP1) into autophagosomes, preventing NFE2L2 ubiquitylation and degradation.[31]

In the study herein, a meta-analysis of sc-RNA-Seq data from six studies from human pancreas islets will be conducted to evaluate how T2DM may modify the transcriptomes of several subpopulations of α- and β-cells. The analysis in total represents sc-RNA-Seq data from 47 metabolically healthy human islet donors and 23 donors with T2DM. Subpopulations of proliferating α-cells, immature, and senescent β-cells will be evaluated using pathway analysis, and gene targets in the NFE2L2 pathway will be

TABLE 1 Dataset accession numbers and sequencing methods

Study	Dataset location and reference numbers	Human donor info	Sequencing methods					Gene annotation methods	
			Cell isolation method	Protocol	Sequencing system	Read length and type	Read depth (reads per cell)	Details	Original unit
Wang et al, 2016[9]	GEO: GSE83139	9 human islets: 3 healthy 2 T2DM 1 T1DM[a] 2 child[a]	Cultured and isolated on a microfluidic system	SMART-seq	Illumina HiSeq 2500	100-bp single-end reads	2.2 million	• Read alignment and quantification performed using RNA-Seq Unified Mapper (RUM)	CPM
Segerstolpe et al, 2016[8]	EBI: E-MTAB-5061	10 human islets: 6 healthy 4 T2DM	Cultured and isolated via FACS	SMART-seq2	Illumina HiSeq 2000	43-bp single-end reads	0.75 million	• Aligned to human genome (hg19) using STAR • Annotated with RefSeq • Quantified using rpkmforgenes	RPKM
Xin et al, 2016[10]	GEO: GSE81608	18 human islets: 12 healthy 6 T2DM	Cultured and isolated using a C1 integrated fluidic circuit	SMART-seq	Illumina HiSeq 2500	75-bp single-end reads	0.95 million	• Aligned to human genome (GRCh37) using CLC Bio Genomics Workbench	RPKM
Baron et al, 2016[5]	GEO: GSE84133	4 human islets: 3 healthy 1 T2DM	Encapsulation into droplets	CEL-seq/MARS-seq	Illumina HiSeq 2500	75-bp paired-end reads	0.1 million	• Read 1 was used for identification • Read 2 was mapped to a ref genome using Bowtie • Alignments were filtered using UMI	TPM
Lawlor et al, 2017[12]	GEO: GSE86473	8 human islets: 5 healthy 3 T2DM	Cultured and isolated via C1 integrated fluidic circuit	SMART-seq2	Illumina NextSeq500	75-bp single-end reads	3 million	• Aligned to the human genome (GRCh37) using Bowtie 2 • Expression levels were estimated using RSEM	TPM
Camunas-Soler et al, 2020[11]	GEO: GSE124742	28 human islets: 18 healthy 7 T2DM 3 T1DM[a]	Isolated via Patch-seq and FACS methods	SMART-seq2	Illumina NextSeq500 or NovaSeq platform	75-bp paired-end reads	1 million	• Aligned to the human genome (GRCh38) using STAR • Gene counts determined using HTSeq-count	CPM

Abbreviations: CPM, normalized counts per million; EBI, European Bioinformatics Institute; FACS, fluorescence-activated cell sorting; GEO, Gene Expression Omnibus; RPKM, reads per kilobase of transcript per million mapped reads; T1DM, type 1 diabetes mellitus; T2DM, type 2 diabetes mellitus; TPM, transcripts per kilobase million.

[a]Donors were excluded.

evaluated in relation to these subpopulations of α- and β-cells. With this analysis, we hope to further understand the role that NFE2L2 may play in T2DM-induced β-cell dysfunction.

2 | METHODS

2.1 | Inclusion criteria

Studies were selected based on PubMed and Google Scholar searches for the key terms "single-cell sequencing," "RNA sequencing," "type 2 diabetes," and "human pancreas or islets." To be included in the meta-analysis, studies had to include (1) single-cell transcriptomic sequencing with (2) human pancreatic islet samples, (3) include metabolically healthy and diabetic donors with T2DM, and (4) provide publicly available annotation data. Publicly available single-cell RNA-seq datasets were downloaded from the Gene Expression Omnibus (GEO) repository[32] or ArrayExpress[33] (European Bioinformatics Institute, EBI), and Table 1 contains study details and accession numbers for selected studies. Before datasets were analyzed, all data were converted to the standard unit of transcripts per kilobase million (TPM). Counts per million reads mapped (CPM) were first converted to reads per kilobase million (RPKM) by dividing CPM by the gene length in kilobase. RPKM values were then converted to TPM by dividing RPKM by the sum of RPKM per sample and multiplying by a 10^6 scaling factor.

2.2 | Cell type annotation

All sequenced cells were classified based on key marker genes. These markers include the major hormone genes (GCG, INS, somatostatin [SST], ghrelin [GHRL], and pancreatic polypeptide [PP]), genes that encode acinar cell-specific digestive enzymes (serine protease 1 [PRSS1] and pancreatic lipase [PNLIP]), and genes associated with ductal cells (i.e., keratin 19 [KRT19], secreted phosphoprotein 1 [SPP1], and hepatocyte nuclear factor 1β [HNF1B]). Expression level of markers had to be exclusive and robust, each cell type was then rendered in a "violin plot," and if cells conflicted with other expression markers, they were excluded.

2.3 | Identification of subpopulations of α- and β-cells

Proliferating α-cells were distinguished by a gene signature with robust expression of marker of proliferation Ki-67 (MKI67), and repression of dual-specificity tyrosine phosphorylation-regulated kinase 1A (DYRK1A) and glycogen synthase kinase 3β (GSK3B), as previously described for proliferating α-cells.[9] Immature β-cells were identified from the pooled dataset by exclusive and robust expression of markers of immaturity, macrophage-activating factor (MAF) basic region-leucine zipper (bZIP) transcription factor B (MAFB) and/or neuropeptide Y (NPY), over markers for mature β-cells (MAF bZIP transcription factor A [MAFA], synaptotagmin 4 [SYT4], NK6 homeobox 1 [NKX6-1], urocortin 3 [UNC3], pancreatic and duodenal homeobox 1 [PDX-1], and glucose transporter 2 [SLC2A2 or GLUT2]) as reviewed by Salinno et al.[16] β-cells were also defined as senescent if they had robust expression of senescent markers, INS-like growth factor 1 receptor (IGF1R), and cyclin-dependent kinase inhibitor 1A and 2A (CDKN1A and CDKN2A).[16] If cells did not have robust expression of any markers, cells were considered unassigned.

2.4 | Differential and meta-analyses

To account for changes within datasets, each dataset was analyzed individually. Within each dataset, a two-tailed Student's *t* test and a permutation-based false discovery rate calculation were used for statistical evaluation of differentially abundant genes for each comparison. *P* values from each dataset were then combined using the mean of each dataset weighted for sample sizes, and a $P < .05$ was considered significant. This technique was selected as it allows for the combination of results from heterogeneous analyses directly. As *P* value-based combination loses the directionality of the expression patterns, fold change values for each dataset were then also combined using the mean of each dataset weighted for sample sizes. Genes not shared across datasets were given values of 1 for both *P* value and fold change calculations.

2.5 | Pathway analysis and individual redox gene expression analysis

Significant genes (*p* value <0.05) and genes with a fold change greater or lower than 20% (ratio of at least −1.2 or 1.2) were selected for pathway analysis using Ingenuity Pathway Analysis (IPA) QIAGEN Bioinformatics (Redwood City, California) to map statistically significant genes to the pathways and biological processes. To explore key genes related to redox signaling, TPM values from all datasets were combined, and a Kruskal-Wallis nonparametric test followed by Dunn's post hoc test for multiple comparisons was performed using GraphPad

Prism v9.1.0 (La Jolla, California) software. Significance was considered to be $p < 0.05$.

3 | RESULTS

3.1 | Cell type identification

α- and β-cells were identified based on exclusive and robust expression of major hormone genes (GCG and INS). Expression levels of all the gene markers were rendered in a "violin plot" (Figure 1A), and if cells had conflicts with other expression markers, they were excluded. After cell types were assigned, 25 genes enriched in α- and β-cells were also evaluated.[8] For α-cells, there was higher expression in α-cell markers, such as transthyretin (TTR) and signal sequence receptor subunit 4 (SSR4), compared to other cell types (Figure 1B.i). For β-cells, there was higher expression in β-cell markers, such as islet amyloid polypeptide (IAPP) and adenylate cyclase-activating polypeptide 1 (ADCYAP1), compared to other cells. (Figure 1B.ii). Overall, 7036 α-cells were identified (2.6% of the α-cells were from Wang et al, 15.0% from Segertolpe et al, 11.8% from Xin et al, 33.1% from Baron et al, 3.4% from Lawlor et al, and 34.2% from Camunas-Soler et al), and 6029 β-cells were identified (1.5% from Wang et al, 7.2% from Segertolpe et al, 6.4% from Xin et al, 41.9% from Baron et al, 4.4% from Lawlor et al, and 38.7% from Camunas-Soler et al) (Figure 1C).

3.2 | α-cell gene expression profiles with T2DM

From the meta-analysis, 285 genes were differentially expressed in α-cells from T2DM donors among the six datasets. Significant genes were then analyzed in IPA. Top significant pathways (z score of <-1.5 or >1.5) and upstream regulators (z score <-2.25 or >2.25), and the top over- and underexpressed genes are listed in Table 2. Overall, α-cells from T2DM donors modified genes involved in energy regulation, autophagy, cell cycle, and xenobiotic metabolism. Additionally, several interleukins were induced in α-cells from T2DM donors, and several hormone signaling pathways were also upregulated, such as β-estradiol and, as expected, INS. The INS secretion signaling pathway was also induced in α-cells from T2DM donors. Of interest to the present study, NFE2L2 was also induced in α-cells from T2DM donors. Several of the top differentially expressed genes (DEGs) were related to energy metabolism, immunity, and peptide hormone metabolism.

3.3 | Proliferating α-cell gene expression profiles

Forty-nine proliferating α-cells were identified from the pooled dataset by exclusive and robust expression of MKI67 vs DYRK1A and GSK3B, and if none of the

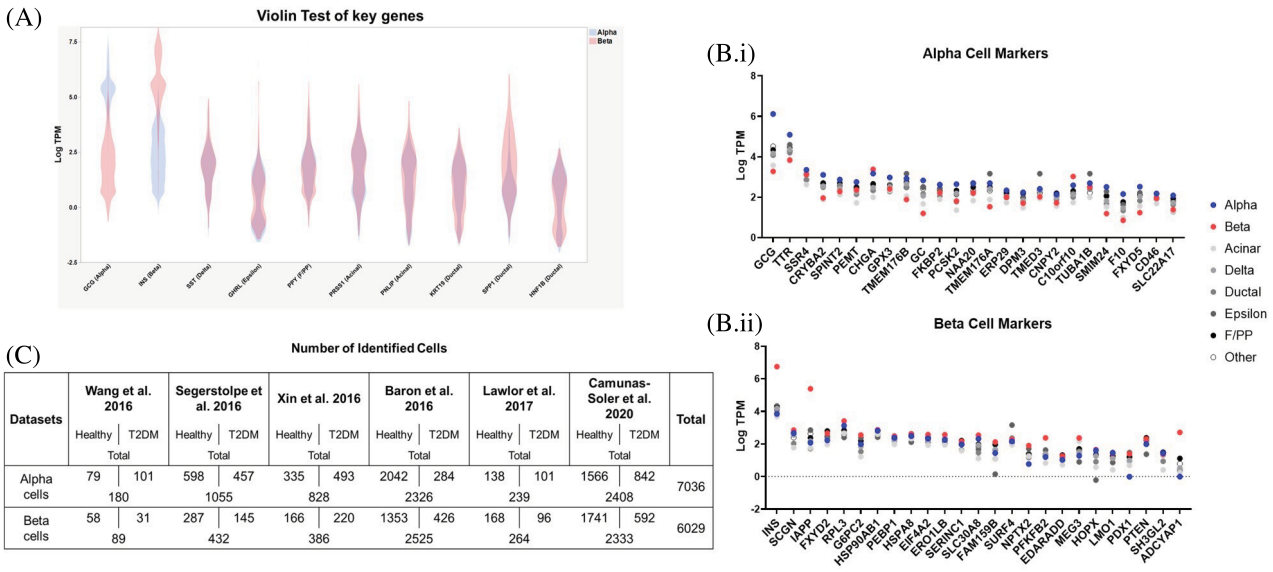

(C) Number of Identified Cells

Datasets	Wang et al. 2016		Segerstolpe et al. 2016		Xin et al. 2016		Baron et al. 2016		Lawlor et al. 2017		Camunas-Soler et al. 2020		Total
	Healthy	T2DM	Healthy	T2DM	Healthy	T2DM	Healthy	T2DM	Healthy	T2DM	Healthy	T2DM	
	Total		Total		Total		Total		Total		Total		
Alpha cells	79	101	598	457	335	493	2042	284	138	101	1566	842	7036
	180		1055		828		2326		239		2408		
Beta cells	58	31	287	145	166	220	1353	426	168	96	1741	592	6029
	89		432		386		2525		264		2333		

FIGURE 1 Cell type identification of integrated dataset s. (A) Violin plot displaying the log-transformed transcripts per million (TPM) of key gene markers in α-(blue) and β-(red) cells. Log-transformed TPM of genes abundantly expressed in α-(B.i) and β-(B.ii) cells are also presented, where each point represents the weighted average among each dataset to account for sample size. (C) The number of cells identified in each dataset based on exclusive and robust expression of key gene markers, number of cells from healthy and diabetic samples are also reported for α-and β-cells

TABLE 2 Type 2 diabetes-driven transcriptomic changes in α-cells

Top canonical pathways			
Name	***z* score**	***P* value**	**Molecules**
Inhibition of ARE-mediated mRNA degradation pathway	−2.000	.0008	CNOT7, PPM1L, PPP2R5C, PPP2R5E, PSMA4, PSMD14
Sirtuin signaling pathway	−1.633	<.0001	ATP5F1B, BAX, GABARAPL1, NDUFA1, NDUFA11, NDUFA13, NDUFB1, NDUFV2, SDHC
EIF2 signaling	1.633	<.0001	ACTB, ATF4, EIF3E, EIF3K, EIF4G2, FAU, RPL12, RPL15, RPL39, RPL4, RPL5, RPS10, RPS2, RPS26, RPS27
Autophagy	1.897	.0008	ATF4, ATM, BIRC6, CALM1, GABARAPL1, GCG, LAMP2, MAPK10, MYD88, PPM1L, PPP2R5C, PPP2R5E
Reelin signaling in neurons	2.000	.0060	ARHGEF12, ARPC1B, ARPC2, MAPK10
Gluconeogenesis I	2.236	<.0001	ALDOA, ENO1, ENO2, GPI, MDH2
Insulin secretion signaling pathway	2.333	.0022	ABCC8, ATF4, CPE, BP2, EIF4G2, GCG, GPAA1, NEUROD1, PK2, PDIA3
Glycolysis I	2.449	<.0001	ALDOA, ENO1, ENO2, GPI, PFKP, PKM
Xenobiotic metabolism PXR signaling pathway	2.449	.0240	ALDH2, ALDH9A1, CITED2, ESD, GSTO2, PPM1A
Xenobiotic metabolism CAR signaling pathway	2.646	.0081	ALDH2, ALDH9A1, CITED2, GSTO2, PPM1L, PPP2R5C, PPP2R5E
Oxidative phosphorylation	3.162	<.0001	ATP5F1B, COX4I1, COX5B, COX7A1, COX8A, NDUFA1, NDUFA11, NDUFA13, NDUFB1, NDUFV2, SDHC
Top upstream regulators			
Upstream regulator	**Name or molecule type**	***z* score**	**Molecules**
RICTOR	Rapamycin-insensitive companion of MTOR	−2.848	ATP5F1B, BAX, COX4I1, COX7A1, COX8A, ENO2, FAU, NDUFA1, NDUFA11, NDUFC1, NDUFC2, NDUFV2, PSMA4, PSMD14, RPL12, RPL4, RPS10, RPS2, RPS26, SDHC
CLPP	Caseinolytic mitochondrial matrix peptidase proteolytic subunit	−2.646	ACADVL, ALDH2, ALDOA, ATP5F1B, ENO1, HSPD1, MDH2, SDHC
TRAP1	TNF receptor-associated protein 1	−2.433	AK3, COX5B, COX8A, HSPD1, NDUFA11, PKM
miR-155-5p	miRNAs w/seed UAAUGCU	−2.407	MATR3, MYD88, MYO10, PICALM, SCAMP1, SO1
NR4A1	Nuclear receptor subfamily 4 group A member 1	−2.335	ALDOA, ATP5F1B, CD36, CTNND1, ENO1, ENO2, EPCAM, GPI, MDH2, NDUFA1, NEUROD1, PDIA3, RPE, SDHC
OSM	Oncostatin M	2.252	ABCC8, ADAM17, ANXA2, ARHGEF12, ASAH1, ATP9A, EPCAM, GFPT1, GRHPR, HLA-A, HLA-B, MYD88, MYH10, RAB4A, RNASE4, SERPINA1, SLC7A8, SNAPC3, SO1, SON
IL15	Interleukin 15	2.255	ALDOA, ATF4, ATM, CALM1 (includes others), CD46, ENO1, ENO2, GDI2, GPI, IL1R1, MACROH2A1, MYD88, OAZ1, PDIA3, PFKP, PKM, PRDX4, RPE, SO1
Insulin	Hormone	2.309	ABCC8, ACAT1, ACOX1, ACTB, ALDOA, CCT4, CCT6A, CCT8, CD36, COX4I1, ENPP2, FKBP2, FTL, GCG, IGFBP2, LGALS3BP, MDH2, NDUFA1, OGT, PKM, PLIN3, PRDX6, PTPRN

(Continues)

TABLE 2 (Continued)

Top upstream regulators			
Upstream regulator	**Name or molecule type**	***z* score**	**Molecules**
IL13	Interleukin 13	2.333	ACADVL, ACOX1, BAX, CAPN2, CD36, ENPP2, IL1R1, PCM1, PFKP, PITRM1, RIN2, SERPINA1, SO1,
CD3	Cluster of differentiation 3	2.335	ATF4, ATM, CALM1 (includes others), COX7A1, FKBP2, FTL, GDI2, HUWE1, IL1R1, MACROH2A1, MDH2, NKTR, OAZ1, PRDX4, RAD23B, SCGN, SNRPB, SNRPN, SO1
TP73	Tumor protein P73	2.382	ADAM17, ATM, BAX, COX4I1, LAPTM4A, SERPINA1
IL5	Interleukin 5	2.383	AK3, ALDOA, ANXA2, ATF4, CITED2, ELL2, ENO1, GCLM, HEPACAM2, MYADM, PDIA6, PFKP, PKM, PRDX4, SO1
SP1	Sp1 transcription factor	2.412	ABCC8, ATM, ATP2A3, ATP5F1B, BAX, CD99, CITED2, FDX1, PKM, BP1, SNRPN, SO1
HSF1	Heat shock transcription factor 1	2.425	BAX, CCT4, CCT6A, CCT8, CD36, DNAJA1, HSPD1, BP1, GAP1
Ige	Immunoglobulin E	2.449	CAPN2, DUSP3, EIF4G2, ENO2, FXYD6, HSPD1, SO1
TCF7L2	Transcription factor 7-like 2	2.522	ASPH, CPD, CREB3L2, ENPP2, EPCAM, GCG, GCLM, IGFBP2, PICALM, REEP3, RNASE4
F2	Coagulation factor II, thrombin	2.630	ADAM17, ATM, BAX, EPCAM, GCH1, GCLM, GLB1, HSPD1, IL1R1, LAMP2, SO1
NFE2L2	Nuclear factor erythroid 2-related factor 2	2.632	ACTG1, ALDOA, ATF4, CD36, CHGB, COX4I1, EIF3E, EIF4G2, ESD, FTL, GCLM, M6PR, MAPK10, NEUROD1, OGT, PDIA3, PDIA6, PFN2, PSMA4, PSMD14, SHMT2, SLC7A8
CAB39L	Calcium-binding protein 39 like	2.646	COX4I1, COX5B, COX8A, NDUFA1, NDUFA13, NDUFC1, NDUFV2
β-estradiol	Hormone	2.711	ABCC8, ACADVL, ACOX1, ACTB, ACTG1, ALDH2, ALDOA, ANKRD12, ANXA2, ARHGEF12, ARPC1B, ASAH1, ATM, ATP5F1B, BAX, CALM1, CAPN2, CDC42BPA, CHGB, CITED2, CTNND1, DUSP3, ENO1, ENPP2, EPB41L3, FUCA1, GCH1, GDI2, GLB1, HLA-A, HSPD1, IGFBP2, IL1R1, KAT6A, LAMP2, LGALS3BP, MAPK10, MYH10, MYH9, MYO10, MYO1B, OAZ1, PDIA3, PKM, PNRC2, PPT1, PRDX4, PTPRN, BP1, RPN2, SCG5, SCGB2A1, SERPINA1, SLC35F3, SLC7A8, SO1
PGR	Progesterone receptor	2.740	ACOX1, AK3, CAPN2, CD36, CDC42BPA, CREB3L2, DST, ELL2, HSPB11, IL1R1, MYO10, PFKP, PFN2, SERPINA1, SIK3
IL4	Interleukin 4	2.827	ACOX1, ACTB, ACTG1, ADAM17, ALDH2, ANXA2, BAX, CD36, CITED2, CLTC, DYNC1H1, HNRNPH3, IL1R1, KIF3A, LAMP2, LGALS3BP, MYH9, NAP1L1, PFKP, PKM, SNRNP200, SO1, SON
IL6	Interleukin 6	3.019	ACOX1, BAX, CD36, CD46, COX4I1, ENO2, ENPP2, GCG, GCH1, HLA-A, IL1R1, MYD88, PCLAF, SERPINA1, SO1
XBP1	X-box-binding protein 1	3.113	ARCN1, ATF4, FKBP2, PDIA3, PDIA6, PGM3, PTPRN, RAB33B, RPN2, SEC63, SERPINA1
AGT	Angiotensinogen	3.423	ACTB, ADAM17, ATP6AP2, BAX, CD36, COX4I1, COX7A1, CPE, FDX1, GCH1, GFPT1, GPC6, IGFBP2, LAMP2, MYH10, SO1

TABLE 2 (Continued)

Top underexpressed genes			Top overexpressed genes		
Gene symbol	**Fold change**	***P* value**	**Gene symbol**	**Fold change**	***P* value**
ASAH1	−1.91	.0223	SLC30A8	5.25	.0463
ATF4	−1.76	.0233	RNASE4	5.22	.0307
SLC35A4	−1.71	.0235	AGPAT2	4.08	.0204
FTL	−1.70	.0324	IVNS1ABP	3.92	.0468
SHMT2	−1.69	.0473	PPP2R3C	3.89	.0459

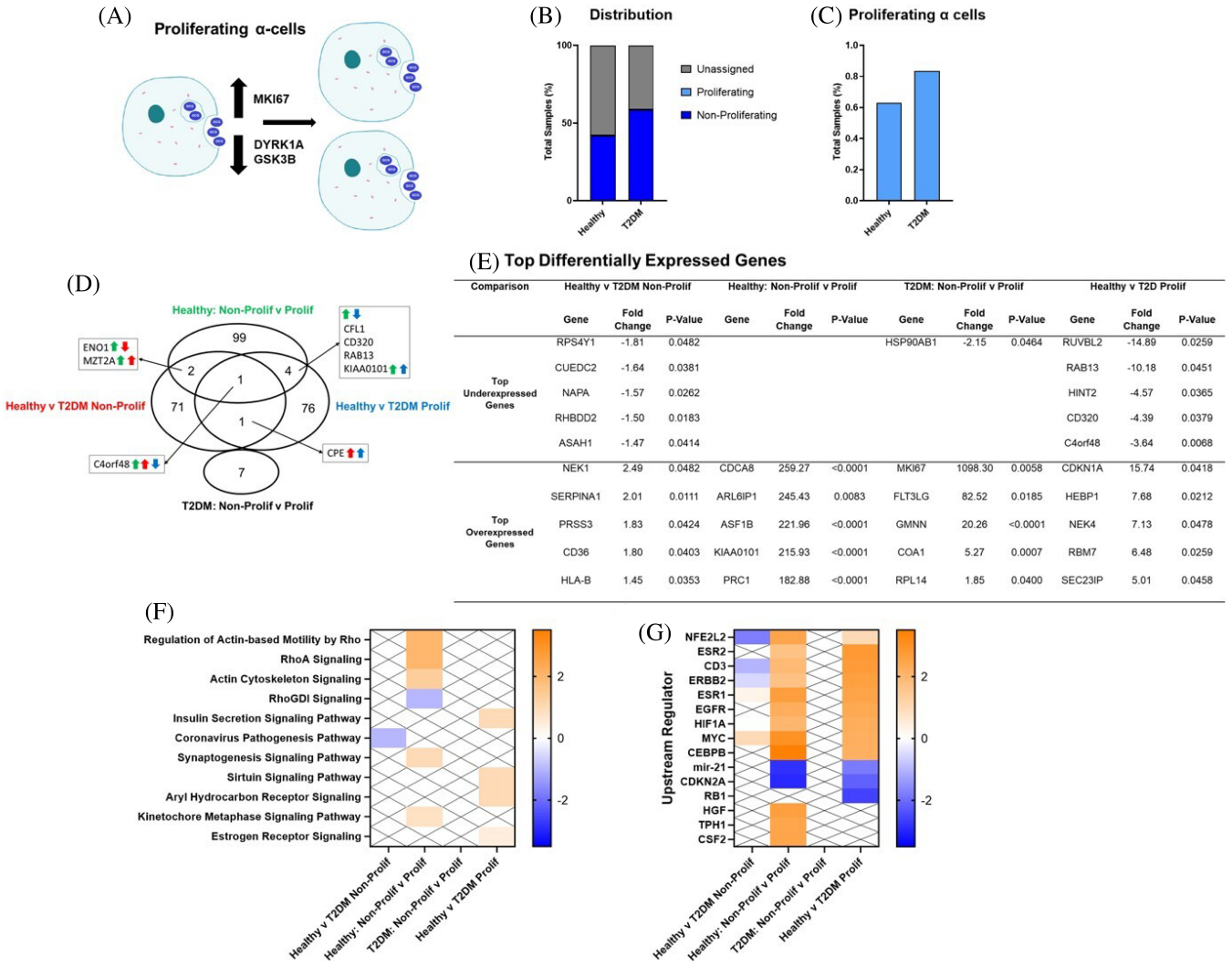

Comparison	Healthy v T2DM Non-Prolif			Healthy: Non-Prolif v Prolif			T2DM: Non-Prolif v Prolif			Healthy v T2D Prolif		
	Gene	Fold Change	P-Value	Gene	Fold Change	P-Value	Gene	Fold Change	P-Value	Gene	Fold Change	P-Value
Top Underexpressed Genes	RPS4Y1	-1.81	0.0482				HSP90AB1	-2.15	0.0464	RUVBL2	-14.89	0.0259
	CUEDC2	-1.64	0.0381							RAB13	-10.18	0.0451
	NAPA	-1.57	0.0262							HINT2	-4.57	0.0365
	RHBDD2	-1.50	0.0183							CD320	-4.39	0.0379
	ASAH1	-1.47	0.0414							C4orf48	-3.64	0.0068
Top Overexpressed Genes	NEK1	2.49	0.0482	CDCA8	259.27	<0.0001	MKI67	1098.30	0.0058	CDKN1A	15.74	0.0418
	SERPINA1	2.01	0.0111	ARL6IP1	245.43	0.0083	FLT3LG	82.52	0.0185	HEBP1	7.68	0.0212
	PRSS3	1.83	0.0424	ASF1B	221.96	<0.0001	GMNN	20.26	<0.0001	NEK4	7.13	0.0478
	CD36	1.80	0.0403	KIAA0101	215.93	<0.0001	COA1	5.27	0.0007	RBM7	6.48	0.0259
	HLA-B	1.45	0.0353	PRC1	182.88	<0.0001	RPL14	1.85	0.0400	SEC23IP	5.01	0.0458

FIGURE 2 Proliferating α-cell gene expression. (A) Proliferating α-cells were distinguished by a gene signature with robust expression of marker of proliferation Ki-67 (MKI67), and repression of dual specificity tyrosine phosphorylation regulated kinase 1A (DYRK1A) and glycogen synthase kinase 3 β-(GSK3B). (B,C) A greater percentage of α-cells from healthy samples (57.59%) were unassigned as compared to T2DM samples (40.69%), X^2 (2, $N = 7036$) = 176.21, $P < .00001$, with Bonferroni correction. (D) Venn diagram illustrating the number of differentially expressed genes (DEGs) detected and shared between comparisons between each comparison between disease and proliferation state. Shared DEGs are listed, and colored arrows indicated direction of each comparison. (E) Top overexpressed and underexpressed differentially expressed gene are listed, including average fold change and *P* value based on each dataset s weighted for sample size. Differentially expressed genes among all comparisons were further analyzed using Ingenuity Pathway Analysis (IPA). Heat-maps describing significant *z*-scores of (F) canonical pathways (≥1.5 or ≤−1.5), and (G) upstream regulators (≥2.25 or ≤−2.25)

target genes were detected, the α-cell was considered unassigned (Figure 2A). A greater percentage of α-cells from healthy donors (57.59%) were unassigned as compared to α-cells from T2DM donors (40.69%), and less than 1% of α-cells were identified as proliferating in the pooled dataset (Figure 2B). Although not significant, the portion of proliferating α-cells from T2DM donors (0.83%) was greater than proliferating α-cells from healthy donors (0.63%) (Figure 2C). There were 75 DEGs in nonproliferating α-cells from T2DM donors, and there were 82 DEGs in proliferating α-cells from T2DM donors (Figure 2D). Carboxypeptidase E (CPE) and neuropeptide-like protein (C4orf48) were the only common DEGs in proliferating and nonproliferating α-cells from T2DM donors and are involved in the biosynthesis of neuropeptides and peptide hormones. There were 106 DEGs in proliferating vs nonproliferating α-cells from healthy donors, and 7 DEGs from T2DM donors. Top DEGs are listed in Figure 2E. In proliferating vs nonproliferating α-cells from T2DM donors, top overexpressed genes included MKI67, a proliferation marker. Most of the top overexpressed genes in proliferating vs nonproliferating α-cells from both healthy and T2DM donors are related to cell division, such as cell division cycle associated 8 (CDCA8). In the pathway analysis (Figure 2F), nonproliferating α-cells from T2DM vs healthy donors repressed the coronavirus pathogenesis pathway. Proliferating α-cells from T2DM vs healthy donors induced the INS secretion signaling pathway and sirtuin signaling pathway similar to results in Table 2. In proliferating α-cells from healthy donors, many of the modulated pathways were related to cell replication, Rho signaling, and in the upstream regulator analysis (Figure 2G), several regulators related to cell proliferation were upregulated, such as proto-oncogene, BHLH transcription factor (MYC). As expected, since the estrogen receptor signaling pathway is induced in proliferating vs nonproliferating α-cells from healthy donors, many of the upstream regulators are related to estrogen signaling. NFE2L2 signaling was induced in proliferating α-cells from healthy donors. In nonproliferating α-cells from T2DM donors, NFE2L2 signaling was repressed; however, in proliferating α-cells from T2DM vs healthy donors, NFE2L2 signaling was induced.

3.4 | β-cell gene expression profiles with T2DM

From our meta-analysis, 286 genes were differentially expressed in β-cells from T2DM donors among the six datasets. Significant genes were then analyzed in IPA, and top significant pathways (z score of <-1.5 or >1.5) and upstream regulators (z score <-2.25 or >2.25), and the top over and underexpressed genes are listed in Table 3. Overall, β-cells from T2DM donors modified genes involved in pathways involved in energy regulation, autophagy, cell cycle, and hormone signaling pathways. As expected with T2DM, the INS secretion signaling pathway was also induced in β-cells from T2DM donors. Again, of interest to the present study, NFE2L2 was induced in β-cells from T2DM donors. Top underexpressed genes include several proteins involved in protein metabolism. IAPP, a β-cell hormone that acts as a satiation signal, is underexpressed in β-cells from T2DM donors. Top overexpressed genes also included SIX homeobox 3 (SIX3). SIX3 represses Wnt activity and activates the sonic hedgehog gene (SHH), and both pathways are involved in β-cell proliferation and differentiation.[34–36]

3.5 | Gene expression profiles of immature β-cells

A total of 2698 immature β-cells were identified from the pooled dataset by exclusive and robust expression of markers of immaturity, MAFB and/or NPY vs markers for mature β-cells (MAFA, SYT4, NKX6-1, UNC3, PDX-1, SLC2A2) (Figure 3A).[16] The portion of immature β-cells from T2DM donors (49.1%) was greater than immature β-cells from healthy donors (43.2%) (Figure 3B). There were 247 DEGs in mature β-cells from T2DM vs healthy donors, and there were 70 DEGs in immature β-cells from T2DM vs healthy donors (Figure 3C). There were 20 common DEGs in both mature and immature β-cells from T2DM vs healthy donors; however, 5 of those genes were induced in mature but decreased in immature β-cells from T2DM donors. In healthy donors, there were 15 DEGs in immature vs mature β-cells, and in T2DM donors, there was 1 DEG in immature vs mature β-cells. NPY, a marker of β-cell immaturity, was overexpressed in mature vs immature β-cells in healthy donors; interestingly, NPY was also overexpressed in immature β-cells from T2DM vs healthy donors (Figure 3D). Similarly, brain-expressed X-linked 1 (BEX1), a top overexpressed gene in immature vs mature β-cells from healthy donors, was also induced in immature β-cells from T2DM vs healthy donors. Another top overexpressed gene in immature vs mature β-cells in healthy donors was glutathione S-transferase omega 1 (GSTO1), a NFE2L2 target gene that activates NF-κB.[37] The only DEG in immature vs mature β-cells from T2DM donors was MAFB, the other maker of β-cell immaturity. In the pathway analysis, as expected, mature and immature β-cells from T2DM vs healthy donors had modified genes involved in

TABLE 3 Type 2 diabetes-driven transcriptomic changes in β-cells

Top canonical pathways			
Name	***z* score**	***P* value**	**Molecules**
Coronavirus pathogenesis pathway	−2.530	<.0001	AGT, CDK4, NUP98, RPS15, RPS2, RPS23, RPS27A, RPS28, RPS3A, RPS4X
Protein kinase A signaling	1.508	.0186	ANAPC13, CALM1 (includes others), CHP1, GNAS, GNB1, MYH10, PRKACB, PRKAR1B, PTEN, PTPRF, SMPDL3A
Gluconeogenesis I	2.000	<.0001	ENO1, ENO2, GAPDH, MDH1
TCA cycle II (eukaryotic)	2.000	.0032	DLD, IDH3G, MDH1, SDHC
Actin cytoskeleton signaling	2.000	.0051	CRKL, ITGAV, MYH10, PFN2, RAC1
Androgen signaling	2.000	.0132	CALM1 (includes others), GNAS, GNB1, GTF2E2, HSP90AA1, POLR2L, PRKACB, PRKAR1B
Oxidative phosphorylation	2.236	<.0001	ATPAF1, COX7A2, NDUFA10, NDUFA13, NDUFB10, NDUFB11 SDHC
Cardiac hypertrophy signaling	2.449	.0182	CALM1 (includes others), CHP1, GNAS, GNB1, PRKACB, PRKAR1B, RAC1
Dopamine-DARPP32 feedback in cAMP signaling	2.646	.0079	ATP2A3, CALM1 (includes others), CHP1, CSNK1A1, GNAS, PPP2R5C, PRKACB, PRKAR1B
Estrogen receptor signaling	2.714	<.0001	AGT, CCNC, CTBP1, DDX5, GNAS, GNB1, HSP90AA1, NDUFA10, NDUFA13, NDUFB10, NDUFB11, NR3C1, PRKACB, PRKAR1B, PTEN, SDHC
EIF2 signaling	3.000	<.0001	EIF1AX, EIF3A, EIF3E, EIF3H, HNRNPA1, RPL11, RPL17, RPL18, RPL18A, RPL26L1, RPL35A, RPL36, RPL37A, RPL38, RPL39, RPL4, RPS15, RPS2, RPS23, RPS27A, RPS28, RPS3A, RPS4X
Autophagy	3.000	.0005	CALM1 (includes others), CHP1, GABARAPL1, GABARAPL2, PPP2R5C, PRKACB, PRKAR1B, PTEN, SESN1
Synaptogenesis signaling pathway	3.051	.0015	AP2M1, CADM1, CALM1 (includes others), CDH1, CHN1, CRKL, HSPA8, NAP1L1, NRXN1, NSF, PRKACB, PRKAR1B, RAC1, RASGRF1
Insulin secretion signaling pathway	3.162	.0110	CLCN3, CPE, DLD, GNAS, NSF, PCSK1, PCSK2, PDX1, PRKACB, PRKAR1B

Top upstream regulators			
Upstream regulator	**Name or molecule type**	***z* score**	**Molecules**
LARP1	La ribonucleoprotein 1, translational regulator	−4.472	EIF3A, EIF3E, EIF3H, EIF4B, HNRNPA1, RPL11, RPL17, RPL18, RPL35A, RPL36, RPL37A, RPL38, RPL39, RPL4, RPS15, RPS2, RPS23, RPS27A, RPS28, RPS3A, RPS4X
NR4A1	Nuclear receptor subfamily 4 group A member 1	−3.000	ACLY, COX7A2, DLD, ENO1, ENO2, EPCAM, MDH1, NDUFA10, NUCB2, PDX1, PEBP1, RAP1GAP2, SDHC, SPINT2
mir-21	miRNA	−2.702	CACYBP, CCT8, CDH1, GPBP1, NUCKS1, PDCD4, PTEN, SESN1
SNAI1	Snail family transcriptional repressor 1	−2.588	CD46, CDH1, CDK4, EPCAM, MLXIPL, PEBP1, PTEN
RICTOR	Rapamycin-insensitive companion of MTOR	−2.559	ATP6V0E2, ATP6V1D, ATP6V1H, COX7A2, ENO2, NDUFA10, NDUFB10, PSMC3, PSMD11, PSMD12, PTEN, RAC1, RPL11, RPL17, RPL18, RPL35A, RPL38, RPL4, RPS15, RPS2, RPS23, RPS27A, SDHC
KDM5A	Lysine-specific demethylase 5A	−2.449	ATP6V1D, COX7A2, MDH1, NDUFA10, NDUFA13, NDUFB10, SDHC
MIR17HG	MiR-17-92a-1 cluster host gene	−2.39	APP, CPE, ECE1, IL6ST, NCSTN, PTEN

(Continues)

TABLE 3 (Continued)

Top upstream regulators			
Upstream regulator	**Name or molecule type**	***z* score**	**Molecules**
NFE2L2	Nuclear factor erythroid 2-related factor 2	2.276	AGT, CCT7, CDH1, DNAJB11, DYNLL1, EIF3E, HSP90AA1, KEAP1, MORF4L2, NUCB2, PFN2, PSMC3, PSMD11, PSMD12, RBBP7, RPL18, SEC23A, SERINC3
FOS	Fructooligosaccharides	2.333	AGT, CADM1, CDH1, CTSB, ENO1, HLA-B, NAE1, NPTX2, NR3C1, PIAS1, PLAGL1, PTS, RBBP7, RPL39
Lh	Luteinizing hormone	2.530	ARL6IP5, CSNK1A1, EIF3H, GNAS, GNB1, POP5, PPP2R5C, PTPRF, RPL17, RPL18A, RPL35A, RPL39, RPS15, RPS2, RPS23, RPS28
PTEN	Phosphatase and tensin homolog	2.583	ACAA2, CCNC, CDH1, CDK4, CLTC, CTSB, CYP27A1, DLD, GAPDH, HMGN1, IDH3G, MDH1, NR3C1, PDCD4, PTEN, PTPRF, RBBP6, SEC23A, SERINC3, SFTPA1, SNX2
ESR1	Estrogen receptor 1	2.72	ACLY, AGT, ALCAM, AP3B1, ARL4D, ATP2A3, ATP6V1H, CCNC, CDH1, CDK4, CLCN3, COPS2, CPE, CRKL, CSNK1A1, CTSB, DDX17, DST, ENO1, EPCAM, GNAS, GNB1, GYG1, HLA-B, HSP90AA1, HSPA13, HSPH1, IL6ST, MAP2, MYH10, NDUFB10, PCM1, PCSK1, PDCD4, PFN2, PGRMC2, PIAS1, PPP2R5C, PRKACB, PRSS23, PTEN, RBP4, RPL18A, RPL38, SCAMP1, SEC31A, SESN1, SMC3, SOCS2
IL5	Interleukin 5	2.813	ACAA2, AK3, ANXA6, ENO1, HSPH1, ITGAV, RAB21, SOCS2
CD3	Cluster of differentiation 3	2.892	CALM1 (includes others), CDK4, CLK1, GABARAPL2, GAPDH, GDI2, GNAS, HMGN1, HNRNPA1, HNRNPR, HSP90AA1, HSPA8, PSAP, PSMD12, PTEN, RPL35A, RPS3A, S100A11, SNRPN, SOCS2, SORL1
PPARG	Peroxisome proliferator-activated receptor gamma	2.934	ACAA2, ACLY, AGT, APP, ARL4D, ATP6V1D, CDH1, ENO2, GABARAPL2, GAPDH, KEAP1, LAPTM4A, MAP2, MDH1, NSF, PDX1, PEPD, PTEN, PTPRF, RBP4, SCP2, SHISA5
CEBPB	CCAAT enhancer-binding protein β	3.072	AGT, APP, CDK4, CIRBP, DDX5, GNAS, HSP90AA1, HSPA8, LGMN, RBBP7, SFTPA1, SMC3
β-estradiol	Hormone	3.302	ACAA2, AGT, ALCAM, ANKRD12, AP3B2, APP, CALM1 (includes others), CDH1, CLCN3, CTSB, DDR1, DDX17, DSP, DYNLL1, EIF3A, ENO1, GDI2, GNB1, GYG1, HNRNPA1, HSPA8, HSPH1, IL6ST, ITGAV, LGMN, MBTPS1, MYH10, NR3C1, NUCB2, PDCD4, PGRMC2, PLAGL1, PRSS23, PSAP, PSMC3, PTEN, RAC1, RASGRF1, RBBP7, RBM39, RBP4, RPL17, S100A11, SCG5, SET, SIX3, SMPDL3A, SOCS2, SPINT2
MYC	MYC proto-oncogene, BHLH transcription factor	3.426	ACLY, ALCAM, ANXA6, APP, CDH1, CDK4, CHP1, CPD, CTSB, DDX5, DSP, ENO1, EPCAM, GAPDH, GDI2, HLA-B, HNRNPA1, HNRNPH1, HNRNPU, HSP90AA1, HSPH1, ITM2B, LGMN, NAP1L1, PDCD4, PEX19, PIAS1, PRKACB, PTEN, RBBP7, RPL11, RPL17, RPL18, RPL18A, RPL35A, RPL37A, RPL38, RPL39, RPL4, RPS15, RPS2, RPS23, RPS27A, RPS28, SCAMP1, SERINC3, SNRPN
MYCN	MYCN proto-oncogene, BHLH transcription factor	3.769	GAPDH, PGRMC2, POLR2L, RBBP7, RPL11, RPL17, RPL18, RPL18A, RPL35A, RPL37A, RPL38, RPL39, RPL4, RPS15, RPS2, RPS23, RPS27A, RPS28, RPS3A, RPS4X
MLXIPL	MLX interacting protein like	3.954	ACLY, MLXIPL, RPL11, RPL17, RPL18, RPL18A, RPL35A, RPL37A, RPL38, RPL39, RPL4, RPS15, RPS2, RPS23, RPS27A, RPS28

TABLE 3 (Continued)

Top underexpressed genes			Top overexpressed genes		
Gene symbol	**Fold change**	***P* value**	**Gene symbol**	**Fold change**	***P* value**
PPP1R1A	−3.24	.0144	SIX3	18.93	0.0153
DNAJB11	−1.92	.0218	SFTPA1	15.08	0.0368
PSMC3	−1.63	.0400	ARL4D	6.34	0.0497
IAPP	−1.62	.0179	HLA-B	5.89	0.0017
ANAPC13	−1.53	.0270	CADM1	5.52	0.0146

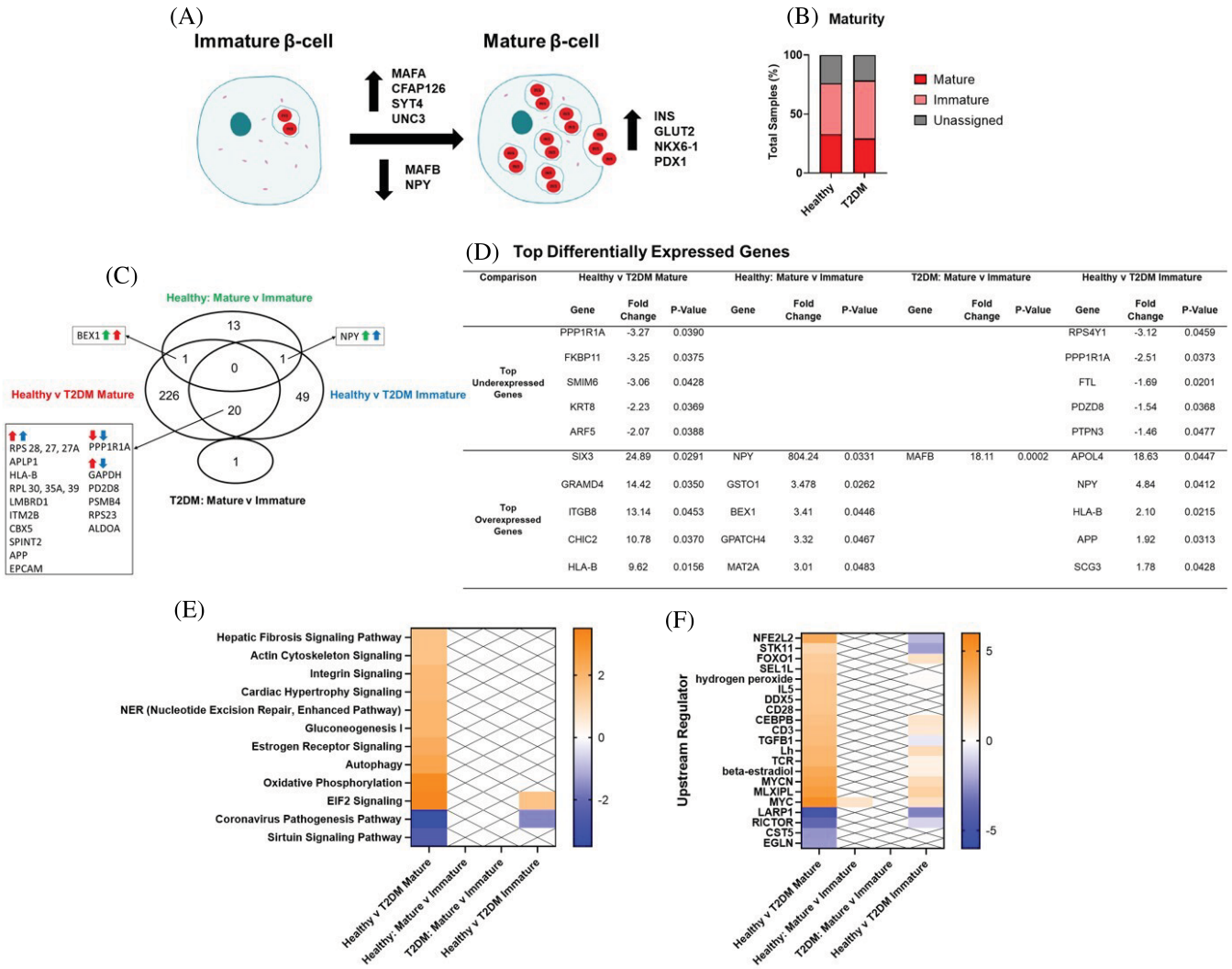

FIGURE 3 Mature and Immature β-cell gene expression. (A) Immature β-cell was defined by exclusive and robust expression of MAFB and/or NPY over markers for mature β-cells (MAFA, SYT4, NKX6-1, UNC3, PDX-1, and SLC2A2). (B) A greater percentage of β-cells from T2DM samples (49.1%) were defined as immature as compared to healthy samples (43.2%), X^2 (2, N = 6028) = 16.29, $P = .0003$, with Bonferroni correction. (C) Venn diagram illustrating the number of differentially expressed genes (DEGs) detected and shared between comparisons between each comparison between disease and maturity. Shared DEGs are listed, and colored arrows indicated direction of each comparison. (D) Top overexpressed and underexpressed differentially expressed gene are listed, including average fold change and *P* value based on each dataset weighted for sample size. Differentially expressed genes among all comparisons were further analyzed using Ingenuity Pathway Analysis (IPA). Heat-maps describing significant *z*-scores of (E) canonical pathways (≥1.5 or ≤−1.5), and (F) upstream regulators (≥2.25 or ≤−2.25)

energy regulation, hormone signaling pathways, and autophagy pathways (Figure 3E,F). There were no pathway changes in mature vs immature β-cells. However, in the upstream regulator analysis, NFE2L2 signaling and STK11 (serine threonine kinase 11), a tumor suppressor, was activated in mature β-cells but downregulated in immature β-cells from T2DM donors. In immature vs mature β-cells from healthy donors, MYC signaling is induced.[38]

3.6 | Gene expression profiles of senescent β-cells

A total of 167 senescent β-cells were identified from the pooled dataset by robust expression of senescent markers IGF1R, CDKN1A, and CDKN2A[16] (Figure 4A). A greater percentage of β-cells from T2DM donors (4.04%) were defined as senescent as compared to β-cells from healthy donors (2.32%) (Figure 4B), and the majority of senescent

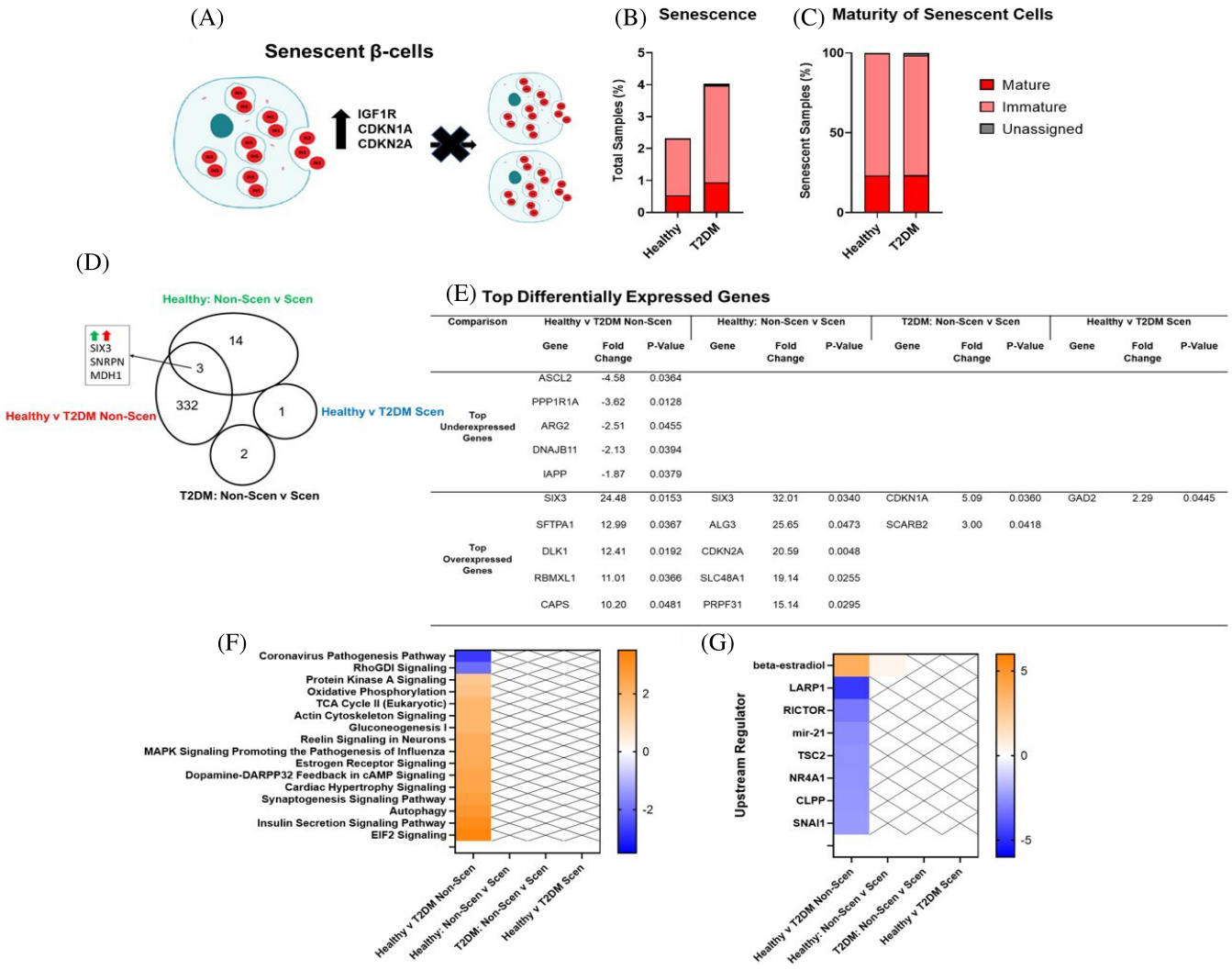

FIGURE 4 Senescent β-cell gene expression. (A) B-cell were also defined as senescent if they had robust expression of senescent markers, IGF1R, CDKN1A, and CDKN1A. (B) A greater percentage of β-cells from T2DM samples (4.04%) were defined as senescent as compared to healthy samples (2.32%), X^2 (1, $N = 6029$) = 12.79, $P = .0003$, with Bonferroni correction. (C) The majority of senescent β-cell were also considered immature, X^2 (4, $N = 6028$) = 25.98, $P = .00003$, with Bonferroni correction. (D) Venn diagram illustrating the number of differentially expressed genes (DEGs) detected and shared between comparisons between each comparison between disease and senescence. Shared DEGs are listed, and colored arrows indicated direction of each comparison. (E) Top overexpressed and underexpressed differentially expressed gene are listed, including average fold change and *P* value based on each dataset s weighted for sample size. Differentially expressed genes among all comparisons were further analyzed using Ingenuity Pathway Analysis (IPA). Heat-maps describing significant *z*-scores of (F) canonical pathways (≥1.5 or ≤ −1.5), and (G) upstream regulators (≥2.25 or ≤−2.25)

β-cells were also considered immature (Figure 4C). There were 335 DEGs in non-senescent β-cells from T2DM vs healthy donors, and there was 1 DEG in senescent β-cells from T2DM vs healthy donors. In healthy donors, there were 17 DEGs in senescent vs non-senescent β-cells, and there were 2 DEGs in senescent β-cells from T2DM donors. The only DEG in senescent β-cells from T2DM vs healthy donors was glutamate decarboxylase 2 (GAD2), a known autoantigen in INS-dependent diabetes (Figure 3D). Additionally, SIX3 is one of the top overexpressed genes in senescent vs non-senescent β-cells from healthy donors and in non-senescent β-cells from T2DM vs healthy donors. In the pathway and upstream regulator analysis, only non-senescent β-cells from T2DM vs healthy sample had significant pathways changes (Figure 4F,G). As expected, both the mature and immature β-cells from T2DM vs healthy donors modified genes involved in energy regulation, hormone signaling pathways, and autophagy pathways.

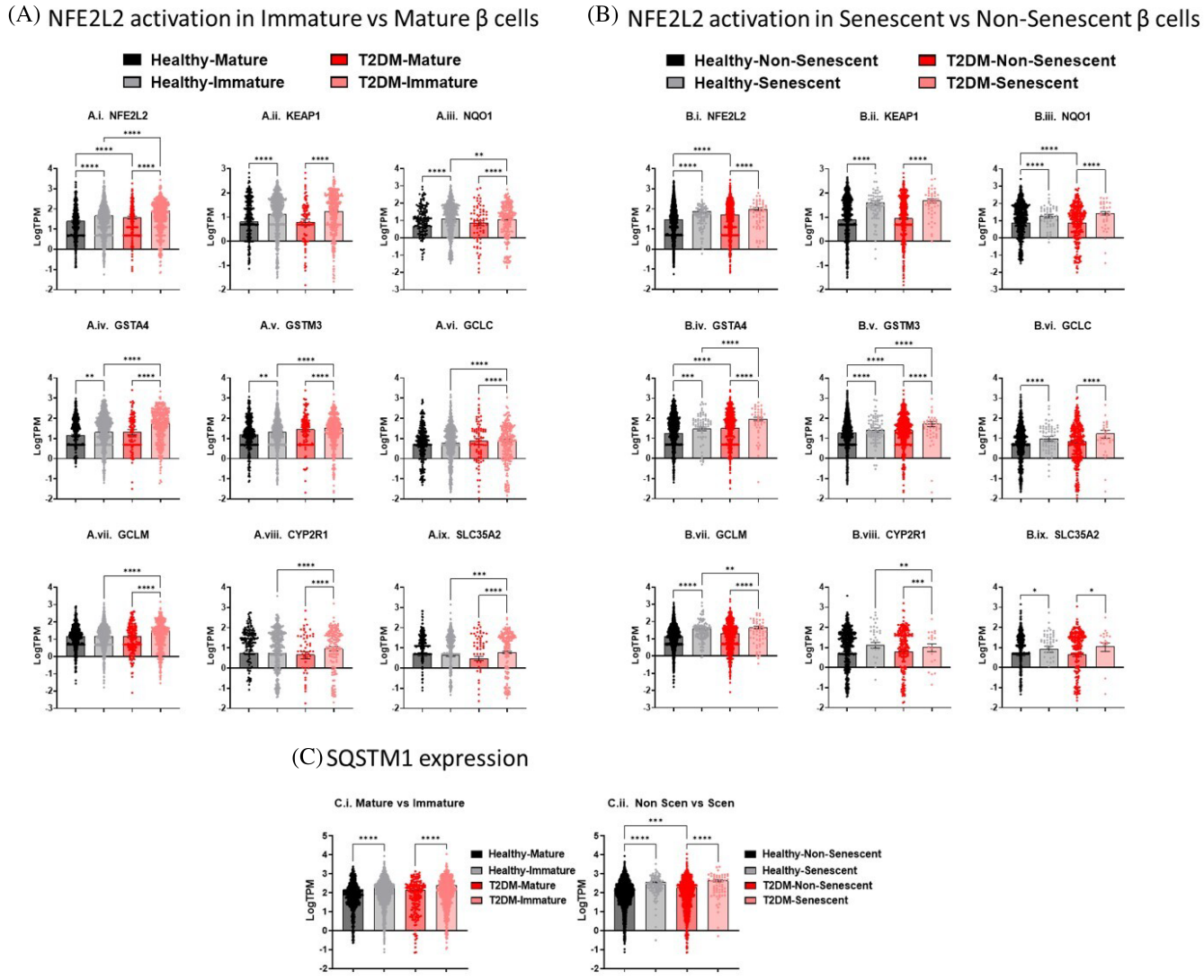

FIGURE 5 NFE2L2 and Redox gene expression. Log transformed transcripts per million (TPM) value of (i) Nuclear factor erythroid 2-related factor 2 (NFE2L2), (ii) Kelch-like ECH-associated protein 1 (KEAP1), (iii) NAD(P)H quinone dehydrogenase 1 (NQO1), (iv) Glutathione S-transferase α-4 (GSTA4), (v) Glutathione S-transferase Mu 3 (GSTM3), (vi) Glutamate-cysteine ligase catalytic subunit (GCLC), (vii) Glutamate-cysteine ligase modifier subunit (GCLM), (viii) Cytochrome P450 2R1 (CYP2R1), and (ix) Solute carrier family 35 member A4 (SLC35A4) were graphed and to evaluate NFE2L2 activation, in (A) immature and (B) senescent β-cells. Additionally, (C) sequestosome 1 (SQSTM1) expression was also evaluated as a possible mechanism of NFE2L2 in (i) immature and (ii) senescent β-cells. All bars represent mean values ± SEM. Calculations were performed using a Kruskal-Wallis nonparametric test, followed by Dunn's post hoc test for multiple comparisons; $N = 1456$ Healthy-Mature, 1920 Healthy-Immature, 465 T2DM-Mature, and 465 T2DM-Immature β-cells and $N = 4340$ Healthy-Non-Senescent, 103 Healthy-Senescent, 1522 T2DM-Non-Senescent, and 64 T2DM-Senescent β-cells. *$P \leq .05$, **$P \leq .01$, ***$P \leq .001$, and ****$P \leq .0001$

3.7 | T2DM activated the NFE2L2 pathway in immature and senescent β-cells

A common upstream regulator that was significantly induced with T2DM was NFE2L2 (Tables 2 and 3). To further evaluate this pathway in relationship to cell dysfunction, several NFE2L2 gene targets were evaluated in α- and β-cells. Proliferating α-cells had minimal changes in selected NFE2L2 gene targets (Figure S1A). Mature β-cells from T2DM donors had increased expression of NFE2L2 by 1.5-fold compared to healthy donors (Figure 5A.i). Immature β-cells from T2DM donors had increased expression of NFE2L2, glutathione S-transferase α-4 (GSTA4), glutathione S-transferase Mu 3 (GSTM3), glutamate-cysteine ligase catalytic subunit (GCLC), glutamate-cysteine ligase modifier subunit (GCLM), cytochrome P450 2R1 (CYP2R1), and solute carrier family 35 member A4 (SLC35A4) by 1.3 to 2.6-fold compared to healthy donors (Figure 5A). In healthy donors, expression of NFE2L2, KEAP1, NAD(P)H quinone dehydrogenase 1 (NQO1), GSTA4, and GSTM3 was induced by 1.3 to 2.7-fold in immature β-cells compared to mature β-cells. However, in the T2DM donors, expression of all the NFE2L2 gene targets evaluated (NFE2L2, KEAP1, NQO1, GSTA4, GSTM3, GCLC, GCLM, CYP2R1, and SLC35A2) was induced by 1.1 to 2.7-fold in immature β-cells vs mature β-cells.

Non-senescent β-cells from T2DM donors had increased expression of NFE2L2, GSTA4, and GSTM3 by 1.8, 1.8, and 1.3-fold, respectively (Figure 5B). Senescent β-cells from the T2DM samples had increased expression of NFE2L2, KEAP1, NQO1, GSTA4, GSTM3, and GCLC; however, the trends were not significant. In healthy and T2DM donors, expression of all the NFE2L2 gene targets (NFE2L2, KEAP1, NQO1, GSTA4, GSTM3, GCLC, GCLM, CYP2R1, and SLC35A2) was induced in senescent β-cells compared to non-senescent β-cells by 1.7 to 5.3-fold.

In addition to the canonical KEAP1 pathway, NFE2L2 can also be activated in a SQSTM1-KEAP1-dependent manner during autophagy dysregulation.[31] SQSTM1 expression is increased by 61.8% and 84.4% in the immature β-cells (Figure 5C.i) and 100.4% and 130.0% in senescent β-cells (Figure 5C.ii) in the healthy and T2DM donors, respectively. Only in the non-senescent β-cells was there a 3% increase in SQSTM1 expression in β-cells from T2DM donors compared to healthy donors.

4 | DISCUSSION

The development of sc-RNA-Seq techniques has allowed for the high-throughput profiling of transcriptomes across cell types and subpopulations of cells and has facilitated understanding of cellular responses to disease.[39] In the present study, a meta-analysis of six sc-RNA-Seq studies from human pancreatic islets was conducted to evaluate the NFE2L2 and redox signaling in α- and β-cells from T2DM vs healthy donors. The transcriptomes of 7036 α-cells and 6029 β-cells were identified and evaluated, and subpopulations of proliferating α-cells, immature, and senescent β-cells were also identified and evaluated.

The modified genes in α-cells from T2DM donors are involved in energy regulation, immune response, xenobiotic metabolism, hormone signaling, and autophagy pathways. In T2DM, α-cells can transdifferentiate to β-cells under an extreme demand for INS,[14] and although not specifically evaluated, an increase in the INS secretion signaling pathway was observed in α-cells from T2DM donors. Forty-nine proliferating α-cells were identified, which represented ~0.7% of identified α-cells. This small percentage is expected as α-cells proliferate at very low levels.[9] As the number of proliferating α-cells was incredibly small, and due to uneven distribution across the datasets, several dataset comparisons were excluded in the meta-analysis when a dataset had only one or no proliferating α-cells. Although the percentage of proliferating α-cells increased in T2DM donors, the trend was not significant (Figure 2C). Previous work has found that IL6, an inflammatory cytokine elevated in T2DM,[40] stimulates α-cell proliferation.[13] Interestingly, in α-cells from T2DM donors, several cytokines, including IL6, IL4, IL5, IL13, and IL15, were identified as upstream regulators. Constant with Wang et al,[9] transcriptomic analysis of proliferating α-cells found modifications in cell cycle pathways. NFE2L2 activation in proliferating α-cells was limited.

Similar to previous sc-RNA-Seq studies, β-cells from T2DM donors have been found to have altered β-cell immune response, cell cycle pathways, energy metabolism, and autophagy pathways.[9–12] The most induced pathway in β-cells from T2DM donors was the INS secretion signaling pathway. In T2DM, there is an increased demand for INS; the increased production of INS in overworked β-cells leads to excessive glucose metabolism and oxidative phosphorylation that increases the generation of ROS.[41] There is also an increase of the unfolding or misfolding of proteins in the ER, leading to ER stress.[42] Oxidative and ER stress can cause apoptotic cell death, which may cause the reduction in β-cell mass that is observed in T2DM.[41–43] As observed herein, pathways and upstream regulators related to apoptosis are induced in β-cells from T2DM donors and include NFE2L2, the master regulator of the antioxidant response. After evaluating the transcriptomes of β-cells from T2DM donors, 2698 immature and 167 senescent β-cells were identified.

β-cells exist in a balance of immature cells and INS-producing mature cells, where the immature cells are thought to reflect proliferative capacity.[16,19] Here, the portion of immature β-cells in T2DM donors was greater than immature β-cells from healthy donors, which is supported by the increase in β-cell proliferation with INS resistance related to obesity.[22] Immature β-cells were defined as an increase in MAFB and/or NPY. Interestingly, NPY was also increased in immature β-cells from T2DM samples vs healthy samples. NPY is a counter-regulator of β-cell INS secretion, and overexpression of NPY in rats has been described to impair INS secretion when fed a high-fat diet.[44,45] In T2DM, there is also an increase in β-cell senescence.[46] Here, a greater percentage of β-cells from T2DM donors were defined as senescent as compared to healthy donors, as defined by expression of senescent markers IGF1R, CDKN1A, and CDKN2A. Remarkably, the majority of senescent β-cells were also considered immature, thus suggesting that senescent β-cells have an increase in either MAFB or NYP expression vs other markers of mature β-cells. SIX3, which represses Wnt activity and activates the SHH,[35] was identified as top overexpressed gene in β-cells from T2DM donors, and SIX3 was also one of the top overexpressed genes in senescent vs non-senescent β-cells. SIX3 has been identified as a transcription factor that governs functional β-cell maturation and may be a potential target for β-cell dysfunction in T2DM.[47]

As outlined in Figure 6, lipotoxicity and glucotoxicity associated with T2DM increase oxidative stress and can increase NFE2L2 activation. As expected, α- and β-cells from T2DM donors have increased NFE2L2 activation. Here, NFE2L2 is also activated in immature and senescent β-cells. Immature β-cells have reduced INS secretion and increased proliferation, and NFE2L2 activation is related to both. Exposure of isolated mouse islets or INS-1 cells to oxidative stressors has been described to decrease glucose-stimulated INS secretion,[48] and upregulation of NFE2L2 expression increases proliferation of rat INS-1 cells and primary mouse and human β-cells.[49,50] Oxidative damage can also damage β-cells, and NFE2L2 was activated in senescent β-cells as well. The pathways analysis demonstrated modified autophagy pathways in cells from T2DM donors, and NFE2L2 activation in β-cells may also occur through the non-canonical SQSTM1-KEAP1 pathway. Here, SQSTM1 expression was increased in immature and senescent β-cells. This suggests that NFE2L2 activation in β-cells is likely due to multiple pathways.

In conclusion, this transcriptomic meta-analysis provides detailed information about β-cell damage in patients with T2DM. These analyses demonstrate the power of sc-RNA-Seq data to detect transcriptional alterations in subpopulations of α- and β-cells. Although the ability to directly relate the changes of the transcriptome to functional impairments in disease is limited, this

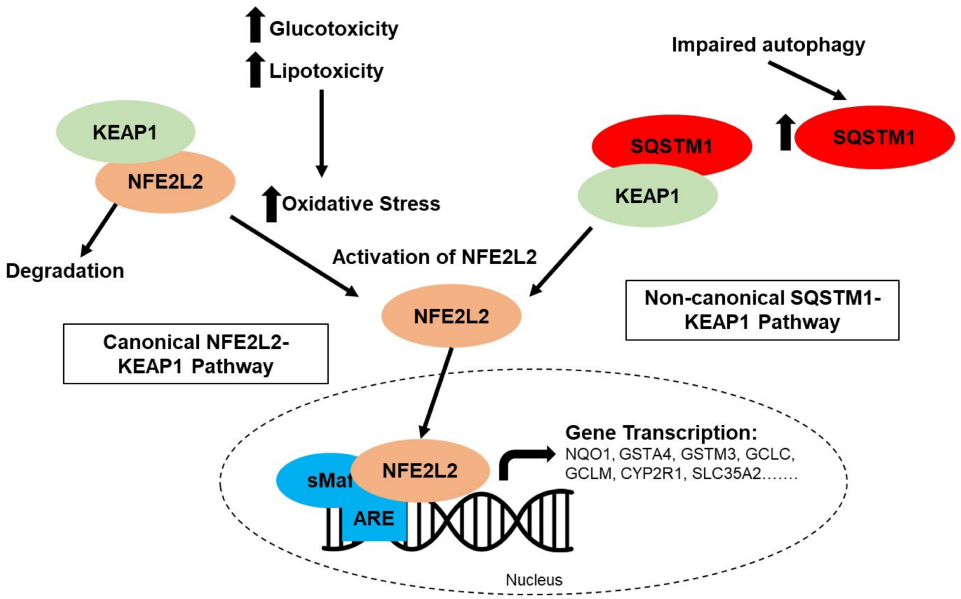

FIGURE 6 Mechanisms of NFE2L2 activation. Under normal conditions, nuclear factor erythroid 2-related factor 2 (NFE2L2) is bound to Kelch-like ECH-associated protein 1 (KEAP1) in the cytoplasm and is degraded. Type 2 diabetes increases glucotoxicity and lipotoxicity, which increases oxidative stress. In the canonical NFE2L2-KEAP1 pathway, when oxidative stress is present, NFE2L2 is activated and translocates to the nucleus. NFE2L2 binds to the antioxidant response element (ARE), along with small Maf (sMaf) proteins to increase expression of antioxidant genes. Sequestosome 1 (SQSTM1) expression is increased with autophagy. In the non-canonical SQSTM1-KEAP1 pathway, SQSTM1 interacts with KEAP1 and inactivates the NFE2L2-KEAP1 complex thus promoting NFE2L2 translocation to the nucleus

analysis provides several hypotheses to understand the effect of T2DM on the α- and β-cells of the pancreas. This study also provides evidence that NFE2L2 activation plays a role in β-cell maturation and dysfunction; redox singling may be a key pathway to target for β-cell restoration and T2DM treatments.

ACKNOWLEDGEMENTS

This work was supported by the National Institute of Health, grant number 5R01ES025748-05 (to A.R.T.-L.). We are grateful to Dr Angela L. Slitt and her laboratory from the University of Rhode Island for providing access to the IPA software purchased from the National Institutes of Health under grant number P42ES027706. The funders had no role in study design, data collection and analysis, decision to publish, or preparation of the manuscript.

DISCLOSURE

The authors have no conflicts of interest, financial or otherwise, to report.

ORCID

Emily Sara Marques https://orcid.org/0000-0001-6819-8154
Alicia R. Timme-Laragy https://orcid.org/0000-0002-8835-5038

REFERENCES

1. Unnikrishnan R, Pradeepa R, Joshi SR, Mohan V. Type 2 diabetes: demystifying the global epidemic. *Diabetes*. 2017;66(6):1432-1442.
2. International Diabetes Federation. IDF Diabetes Atlas, 9th edn. Brussels, Belgium; 2019. Available at: https://diabetesatlas.org
3. El Sayed SA, Mukherjee S. Physiology, pancreas. *StatPearls*. Treasure Island, FL: StatPearls Publishing; 2021.
4. Tritschler S, Theis FJ, Lickert H, Böttcher A. Systematic single-cell analysis provides new insights into heterogeneity and plasticity of the pancreas. *Mol Metab*. 2017;6(9):974-990.
5. Baron M, Veres A, Wolock SL, et al. A single-cell transcriptomic map of the human and mouse pancreas reveals inter- and intra-cell population structure. *Cell Syst*. 2016;3(4):346-360.e4.
6. Enge M, Arda HE, Mignardi M, et al. Single-cell analysis of human pancreas reveals transcriptional signatures of aging and somatic mutation patterns. *Cell*. 2017;171(2):321-330.e14.
7. Muraro MJ, Dharmadhikari G, Grün D, et al. A single-cell transcriptome atlas of the human pancreas. *Cell Syst*. 2016;3(4):385-394.e3.
8. Segerstolpe Å, Palasantza A, Eliasson P, et al. Single-cell transcriptome profiling of human pancreatic islets in health and type 2 diabetes. *Cell Metab*. 2016;24(4):593-607.
9. Wang YJ, Schug J, Won K-J, et al. Single-cell transcriptomics of the human endocrine pancreas. *Diabetes*. 2016;65(10):3028-3038.
10. Xin Y, Kim J, Okamoto H, et al. RNA sequencing of single human islet cells reveals type 2 diabetes genes. *Cell Metab*. 2016;24(4):608-615.
11. Camunas-Soler J, Dai X-Q, Hang Y, et al. Patch-Seq links single-cell transcriptomes to human islet dysfunction in diabetes. *Cell Metab*. 2020;31(5):1017-1031.e4.
12. Lawlor N, George J, Bolisetty M, et al. Single-cell transcriptomes identify human islet cell signatures and reveal cell-type–specific expression changes in type 2 diabetes. *Genome Res*. 2017;27(2):208-222.
13. Ellingsgaard H, Ehses JA, Hammar EB, et al. Interleukin-6 regulates pancreatic α-cell mass expansion. *Proc Natl Acad Sci U S A*. 2008;105(35):13163-13168.
14. Thorel F, Népote V, Avril I, et al. Conversion of adult pancreatic alpha-cells to beta-cells after extreme beta-cell loss. *Nature*. 2010;464(7292):1149-1154.
15. Chung C-H, Levine F. Adult pancreatic alpha-cells: a new source of cells for beta-cell regeneration. *Rev Diabet Stud*. 2010;7(2):124-131.
16. Salinno C, Cota P, Bastidas-Ponce A, Tarquis-Medina M, Lickert H, Bakhti M. β-cell maturation and identity in health and disease. *Int J Mol Sci*. 2019;20(21):5417.
17. Szabat M, Page MM, Panzhinskiy E, et al. Reduced insulin production relieves endoplasmic reticulum stress and induces β cell proliferation. *Cell Metab*. 2016;23(1):179-193. https://doi.org/10.1016/j.cmet.2015.10.016
18. Helman A, Klochendler A, Azazmeh N, et al. p16(Ink4a)-induced senescence of pancreatic beta cells enhances insulin secretion. *Nat Med*. 2016;22(4):412-420.
19. Puri S, Roy N, Russ HA, et al. Replication confers β cell immaturity. *Nat Commun*. 2018;9(1):485.
20. Blum B, Hrvatin S, Schutz C, Bonal C, Rezaniaand A, Melton DA. Functional β-cells maturation is marked by an increase in the glucose threshold for insulin secretion and by expression of urocortin3. *Nat Biotechnol*. 2012;30(3):261-264.
21. Dorrell C, Schug J, Canaday PS, et al. Human islets contain four distinct subtypes of β cells. *Nat Commun*. 2016;7(1):11756.
22. Linnemann AK, Baan M, Davis DB. Pancreatic β-cell proliferation in obesity. *Adv Nutr*. 2014;5(3):278-288.
23. Burgos-Morón E, Abad-Jiménez Z, Martínez de Marañón A, et al. Relationship between oxidative stress, ER stress, and inflammation in type 2 diabetes: the battle continues. *J Clin Med*. 2019;8(9):1385.
24. Wang J, Wang H. Oxidative stress in pancreatic Beta cell regeneration. *Oxid Med Cell Longev*. 2017;2017:e1930261.
25. Miki A, Ricordi C, Sakuma Y, et al. Divergent antioxidant capacity of human islet cell subsets: a potential cause of beta-cell vulnerability in diabetes and islet transplantation. *PLoS One*. 2018;13(5):e0196570.
26. Rastogi A, Severance EG, Jacobs HM, Conlin SM, Islam ST, Timme-Laragy AR. Modulating glutathione thiol status alters pancreatic β-cell morphogenesis in the developing zebrafish (Danio rerio) embryo. *Redox Biol*. 2021;38:101788.
27. Lenzen S, Drinkgern J, Tiedge M. Low antioxidant enzyme gene expression in pancreatic islets compared with various other mouse tissues. *Free Radic Biol Med*. 1996;20(3):463-466.
28. Liang J, Wu SY, Zhang D, Wang L, Leung KK, Leung PS. NADPH oxidase-dependent reactive oxygen species stimulate β-cell

regeneration through differentiation of endocrine progenitors in murine pancreas. *Antioxid Redox Signal*. 2016;24(8):419-433. https://doi.org/10.1089/ars.2014.6135
29. Ahmed Alfar E, Kirova D, Konantz J, Birke S, Mansfeld J, Ninov N. Distinct levels of reactive oxygen species coordinate metabolic activity with beta-cell mass plasticity. *Sci Rep*. 2017; 7(1):3994.
30. Pi J, Zhang Q, Fu J, et al. ROS signaling, oxidative stress and Nrf2 in pancreatic beta-cell function. *Toxicol Appl Pharmacol*. 2010;244(1):77-83.
31. Lau A, Wang X-J, Zhao F, et al. A noncanonical mechanism of Nrf2 activation by autophagy deficiency: direct interaction between Keap1 and p62. *Mol Cell Biol*. 2010;30(13):3275-3285.
32. Barrett T, Wilhite SE, Ledoux P, et al. NCBI GEO: archive for functional genomics dataset s—update. *Nucleic Acids Res*. 2013; 41(D1):D991-D995. https://doi.org/10.1093/nar/gks1193
33. Athar A, Füllgrabe A, George N, et al. ArrayExpress update – from bulk to single-cell expression data. *Nucleic Acids Res*. 2019;47(D1):D711-D715.
34. Thomas MK, Rastalsky N, Lee JH, Habener JF. Hedgehog signaling regulation of insulin production by pancreatic beta-cells. *Diabetes*. 2000;49(12):2039-2047.
35. Carlin D, Sepich D, Grover VK, Cooper MK, Solnica-Krezel L, Inbal A. Six3 cooperates with Hedgehog signaling to specify ventral telencephalon by promoting early expression of Foxg1a and repressing Wnt signaling. *Development*. 2012;139(14):2614-2624.
36. Chen J, Ning C, Mu J, Li D, Ma Y, Meng X. Role of Wnt signaling pathways in type 2 diabetes mellitus. *Mol Cell Biochem*. 2021;476(5):2219-2232.
37. Board PG, Menon D. Structure, function and disease relevance of omega-class glutathione transferases. *Arch Toxicol*. 2016; 90(5):1049-1067.
38. Rosselot C, Kumar A, Lakshmipathi J, et al. Myc is required for adaptive β-cell replication in young mice but is not sufficient in one-year-old mice fed with a high-fat diet. *Diabetes*. 2019; 68(10):1934-1949.
39. Sandberg R. Entering the era of single-cell transcriptomics in biology and medicine. *Nat Methods*. 2014;11(1):22-24.
40. Bowker N, Shah RL, Sharp SJ, et al. Meta-analysis investigating the role of interleukin-6 mediated inflammation in type 2 diabetes. *EBioMedicine*. 2020;61:103062.
41. Baumel-Alterzon S, Katz LS, Brill G, Garcia-Ocaña A, Scott DK. Nrf2: the master and captain of beta cell fate. *Trends Endocrinol Metab*. 2021;32(1):7-19.
42. Meyerovich K, Ortis F, Allagnat F, Cardozo AK. Endoplasmic reticulum stress and the unfolded protein response in pancreatic islet inflammation. *J Mol Endocrinol*. 2016;57(1):R1-R17.
43. Elksnis A, Martinell M, Eriksson O, Espes D. Heterogeneity of metabolic defects in type 2 diabetes and its relation to reactive oxygen species and alterations in beta-cell mass. *Front Physiol*. 2019;10:107.
44. Machida Y, Bruinsma C, Hallinger DR, et al. Pancreatic islet neuropeptide Y overexpression has minimal effect on islet morphology and β-cell adaptation to high-fat diet. *Endocrinology*. 2014;155(12):4634-4640. https://doi.org/10.1210/en.2014-1537
45. Yang C-H, Onda D-A, Oakhill JS, Scott JW, Galic S, Loh K. Regulation of pancreatic β-cell function by the NPY system. *Endocrinology*. 2021;162(8):1-8.
46. Aguayo-Mazzucato C, Andle J, Lee TB, et al. Acceleration of β cell aging determines diabetes and senolysis improves disease outcomes. *Cell Metab*. 2019;30(1):129-142.e4.
47. Bevacqua RJ, Lam JY, Peiris H, et al. SIX2 and SIX3 coordinately regulate functional maturity and fate of human pancreatic β cells. *Genes Dev*. 2021;35(3–4):234-249.
48. Pi J, Bai Y, Zhang Q, et al. Reactive oxygen species as a signal in glucose-stimulated insulin secretion. *Diabetes*. 2007;56(7):1783-1791.
49. Kumar A, Katz LS, Schulz AM, et al. Activation of Nrf2 is required for normal and ChREBPα-augmented glucose-stimulated β-cell proliferation. *Diabetes*. 2018;67(8):1561-1575.
50. Yagishita Y, Fukutomi T, Sugawara A. et al. Nrf2 protects pancreatic β-cells from oxidative and nitrosative stress in diabetic model mice. *Diabetes*. 2014;63(2):605-618. https://doi.org/10.2337/db13-0909

SUPPORTING INFORMATION

Additional supporting information may be found in the online version of the article at the publisher's website.

How to cite this article: Marques ES, Formato E, Liang W, Leonard E, Timme-Laragy AR. Relationships between type 2 diabetes, cell dysfunction, and redox signaling: A meta-analysis of single-cell gene expression of human pancreatic α- and β-cells. *Journal of Diabetes*. 2022;14(1):34-51. doi:10.1111/1753-0407.13236